Structure of Plasma Heating in Gyrokinetic Alfvénic Turbulence

Alejandro Bañón Navarro,[1, *] Bogdan Teaca,[2, †] Daniel Told,[1] Daniel Groselj,[1, 3] Paul Crandall,[1] and Frank Jenko[1]

[1]*Department of Physics and Astronomy, UCLA, 475 Portola Plaza, Los Angeles, CA 90095-1547, USA*
[2]*Applied Mathematics Research Centre, Coventry University, Coventry CV1 5FB, United Kingdom*
[3]*Max-Planck-Institut für Plasmaphysik, Boltzmannstraße 2, D-85748 Garching, Germany*

We analyze plasma heating in weakly collisional kinetic Alfvén wave turbulence using high resolution gyrokinetic simulations spanning the range of scales between the ion and the electron gyroradii. Real space structures that have a higher than average heating rate are shown not to be confined to current sheets. This novel result is at odds with previous studies, which use the electromagnetic work in the local electron fluid frame, i.e. $\mathbf{J} \cdot (\mathbf{E} + \mathbf{v}_e \times \mathbf{B})$, as a proxy for turbulent dissipation to argue that heating follows the intermittent spatial structure of the electric current. Furthermore, we show that electrons are dominated by parallel heating while the ions prefer the perpendicular heating route. We comment on the implications of the results presented here.

Introduction.— The radial temperature profile of the solar wind, as measured by spacecraft, can only be explained by the presence of heating throughout the heliosphere [1]. Identifying the physical mechanisms that dissipate small-scale turbulent fluctuations, ultimately converting the turbulent energy into heat, is thus one of the major unsolved problems in the solar wind community [2]. Due to the low collisionality of the solar wind, a kinetic model is necessary to understand the effects that contribute to the heating of the plasma. Over the past years, a major effort has been put into computational studies of the problem using fully kinetic and reduced kinetic models in two or three spatial dimensions [3–15].

Recent kinetic plasma simulations found that the dissipation of electromagnetic turbulent fluctuations occurs in an intermittent hierarchy of coherent structures [7–10, 13, 14], confirming a series of solar wind satellite observations [16–21]. This led to the conjecture that heating in turbulent space plasmas is also highly inhomogeneous, patchy and occurs predominantly in current sheets. However, to date, fully kinetic simulations in two or three spatial dimensions do not compute the actual local heating rate, depending instead on a number of proxies [10, 13]. The electromagnetic work on the plasma particles in the fluid frame represents the most common proxy for heating in a weakly collisional turbulent plasma.

This work addresses for the first time in a direct way the real space structure of heating in weakly collisional kinetic Alfvén wave (KAW) turbulence, which has been demonstrated to be a crucial ingredient of solar wind turbulence [22–25]. In this context, a series of questions emerge. Does the plasma heating occur predominantly in current sheets or not? How much of the structure exhibited by collisional heating can be captured by electromagnetic work and how appropriate is the latter as a dissipation proxy for turbulent heating? Is the heating more homogeneous, or does it have a patchy nature? What are the main mechanisms for turbulent heating and do they occur predominantly in the perpendicular or parallel direction in velocity space? We provide answers to these questions before commenting on the implications of the results found in the broader context of solar wind research.

Simulation setup.— In this work, KAW turbulence is stud-

ied using the gyrokinetic (GK) theory [26], which is a rigorous limit of kinetic theory in strongly magnetized plasmas. It assumes low frequencies (compared to the ion cyclotron frequency) and small fluctuation levels. Therefore, it excludes cyclotron resonances and stochastic heating. A recent comparison [27] with the fully kinetic model found that GK is able to accurately reproduce the physics of KAWs for the parameters considered in this study. Furthermore, the reduction of the problem to a five-dimensional phase space allows for the use of a realistic mass ratio and a grid-based numerical scheme, which does not suffer from discrete particle noise and is able to treat heating explicitly via a well-defined collision operator. To date, several previous works have considered the plasma heating problem in three-dimensional turbulence using GK theory [6, 8]. However, none of these studies has measured directly the collisional dissipation in real space.

The data used in this Letter is taken from the simulation presented in Ref. [6], and it is briefly summarized in the following. The nonlinear gyrokinetic system of equations is solved with the Eulerian code GENE [28], capturing the dynamics of KAW turbulence in three spatial dimensions. A magnetic antenna potential amplitude, evolved in time according to a Langevin equation [29], is externally prescribed at the largest scale of the simulation to model the energy injection at the outer scales of the system. The driven modes in units of the lowest wave numbers in (k_x, k_y, k_z) are $(0, 1, \pm 1)$ and $(1, 0, \pm 1)$. The modes are driven using a mean antenna frequency $\omega_a = 0.9\,\omega_{A0}$, decorrelation rate $\gamma_a = 0.7\,\omega_{A0}$, and amplitude $A_{\parallel,0} = \omega_{A0} B_0 / (\sqrt{2}\,k_{\perp,0}^2 v_A)$, where ω_{A0} is the frequency of the slowest Alfvén wave in the system. Compared to Ref. [6] we filter out the antenna wavenumber modes when computing our diagnostics. We chose physical parameters of the simulation to be close to the solar wind conditions at 1 AU, with $\beta_i = 8\pi n_i T_i / B_0^2 = 1$ and $T_i/T_e = 1$. Proton and electron species are included with their real mass ratio of $m_i/m_e = 1836$. Electron collisionality is chosen to be $\nu_e = 0.06\,\omega_{A0}$ (with $\nu_i = \sqrt{m_e/m_i}\nu_e$). The evolution of the gyrocenter distribution is tracked on a grid with resolution $(N_x, N_y, N_z, N_{v_\parallel}, N_\mu, N_\sigma) = (768, 768, 96, 48, 15, 2)$. The resolution covers a perpendicular wave number range of
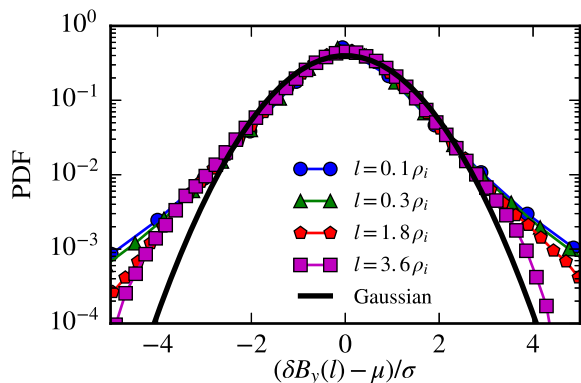
FIG. 1. (Color online) PDFs of magnetic field increments for different separation lengths l. The increments are normalized by their standard deviations (σ) and the averages (μ) were subtracted before computing the PDFs.

$0.2 \leq k\rho_i \leq 51.2$ (or $0.0047 \leq k_\perp \rho_e \leq 1.19$). Here, $\rho_\sigma = \sqrt{T_\sigma m_\sigma} c/eB_0$ is the species gyroradius and σ denotes the species type. The range of wave numbers covered corresponds to a perpendicular box size of $L_\perp = 10\pi\rho_i$ (the equivalent of roughly 44 ion inertial lengths). In the dynamically fully developed state, the turbulent fields display strong intermittent fluctuations, which can be examined by calculating the probability density function (PDF) of field increments for various lags in directions perpendicular to the mean magnetic field. In Fig. 1, we analyze the PDFs of magnetic field increments $\delta B_y(l) = B_y(\vec{r} + \vec{l}) - B_y(\vec{r})$ for different separation lengths l. We observe that the increments at large separation approach a Gaussian, while the increments at small separations develop increasingly strong non-Gaussian tails, indicating intermittency [30].

Plasma heating and dissipation measures.— Boltzmann's H-Theorem states that any increase in entropy, necessary for irreversible heating, can only occur due to collisions [31]. For this reason, in the context of this paper heating refers to the collisional dissipation of GK turbulence, for which the free energy represents a measure of the intensity of turbulent fluctuations. The collisional dissipation rate for each plasma species is defined in real space (x, y, z) at a given time t as

$$Q_\sigma(x, y, z, t) = \frac{2\pi B_0}{m_\sigma} \int dv_\parallel d\mu \frac{T_\sigma}{F_{0,\sigma}} h_\sigma C[f_\sigma]. \quad (1)$$

Here, $F_{0,\sigma}$ is a Maxwellian background distribution with background density n_σ and temperature T_σ, f_σ is the perturbed GK distribution function, and h_σ its nonadiabatic part. The nonadiabatic part is given by $h_\sigma = f_\sigma + (q_\sigma \bar{\phi}_{1,\sigma} + \mu \bar{B}_{1,\parallel\sigma}) F_{0,\sigma}/T_\sigma$, where ϕ and $B_{1,\parallel\sigma}$ are, respectively, the self-consistent electrostatic and parallel magnetic field up to first order and the over-bar refers to a gyro-average. The collision operator $C[f_\sigma]$ is of a linearized Landau-Boltzmann [32] type with energy and momentum conserving terms (see Supplemental Material [33] for an explicit form of the collision operator implemented in GENE). Finally, the total plasma collisional dissipation rate is obtained as a sum of contributions

from the two species ($Q = \sum_\sigma Q_\sigma$). For the parameters used in this work, the electron collisional dissipation peaks in the interval $1 < k_\perp \rho_i < 10$, while the ion collisional dissipation peaks in the $10 < k_\perp \rho_i < 50$ interval. More importantly, about 70% of the total collisional dissipation is found to arise from electron collisions.

The perturbed part of the distribution function is assumed small here ($f_\sigma \ll F_{0,\sigma}$). Hence, collisions are accurately described by a linearized collision operator within this approximation, whereas large fluctuations in f_σ would require the use of a nonlinear operator [34, 35]. While neglecting large fluctuations, our model still captures an essential feature of (weakly) collisional dissipation, that is, heating is increased locally due to large velocity gradients in the perturbed distribution function. As small velocity scales develop naturally in the weakly collisional limit through kinetic effects, such as linear Landau damping and nonlinear phase mixing, the small scale velocity gradients contribute more and more to the heating of the plasma. It is also worth emphasizing that the collision frequency for this study was chosen sufficiently low so as not to limit the kinetic range physics contained in the GK model. Therefore, collisionality should be understood as an ultimate sink for free energy that prevents unlimited filamentation of structures in velocity space while still allowing for a broad range of kinetic effects.

We compare the local heating rates to the so-called electron frame dissipation measure (EFDM) [36]

$$D_e = \mathbf{J} \cdot (\mathbf{E} + \mathbf{v}_e \times \mathbf{B}), \quad (2)$$

where $\mathbf{v}_e$ the electron fluid velocity. The standard definition of D_e contains a second term proportional to the charge density, which is cancelled out by the quasineutrality assumption made here. The EFDM is related to the work done by the non-ideal part of the electric field in the generalized Ohm's law ($\propto J^2$ in resistive MHD) and it is the same in the electron and ion frame when quasineutrality is assumed [10]. Several authors have recently considered D_e as a proxy for turbulent dissipation in situations where no explicit expression for collisional dissipation is available [10, 13, 17]. Hereafter, we will consider only $D_e > 0$ since this is where the energy is taken out of the electromagnetic fields.

Relation of current sheets to heating and the EFDM.— We observe that the current is distributed in a hierarchy of structures: smooth sheets that are twisted in large scale vortices coexist with smaller scale filaments (Fig. 2). The real space structure of ion and electron heating differs. While Q_i is more uniform, Q_e clearly shows a patchy nature. For a given z plane at a given instant in time, we define current sheets as regions of high current that exceed the space-averaged root-mean-square (RMS) value $J^{rms} = \langle J^2 \rangle^{1/2}$. Similarly, we look at regions of high heating rates, for which $|Q_\sigma(x, y)| \geq Q_\sigma^{rms}$. For electrons, these structures contribute to about 50% of the total electron heating. Already this fact alone demonstrates that a significant amount of the electron heating cannot be attributed to regions with intense peaks in the heating, even though a patchy nature for Q_e is evident
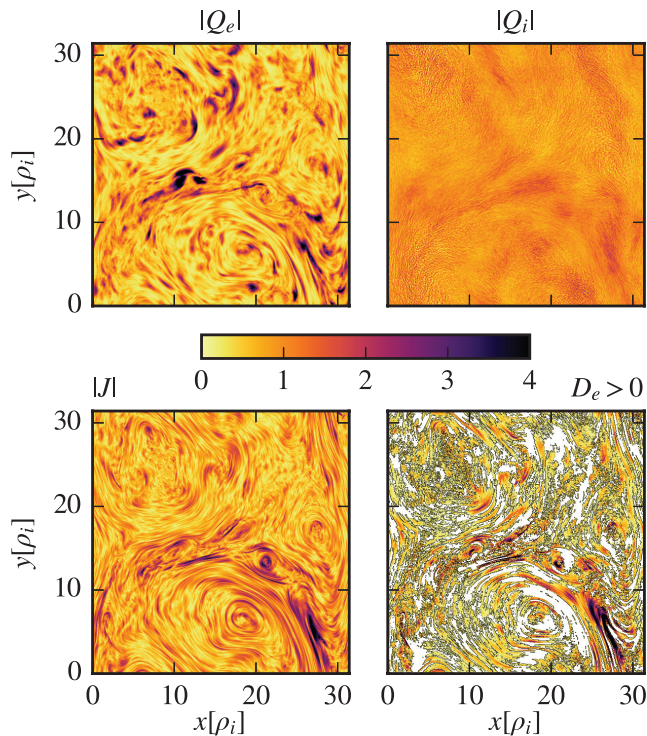
FIG. 2. (Color online) Magnitude of the electron and ion heating density, current density, and the EFDM for a given z plane at a given instant in time. The fields have been normalized to their RMS values and values exceeding the range $[0,4]$ have been clipped to the bounding values of the chosen color (gray) scale.
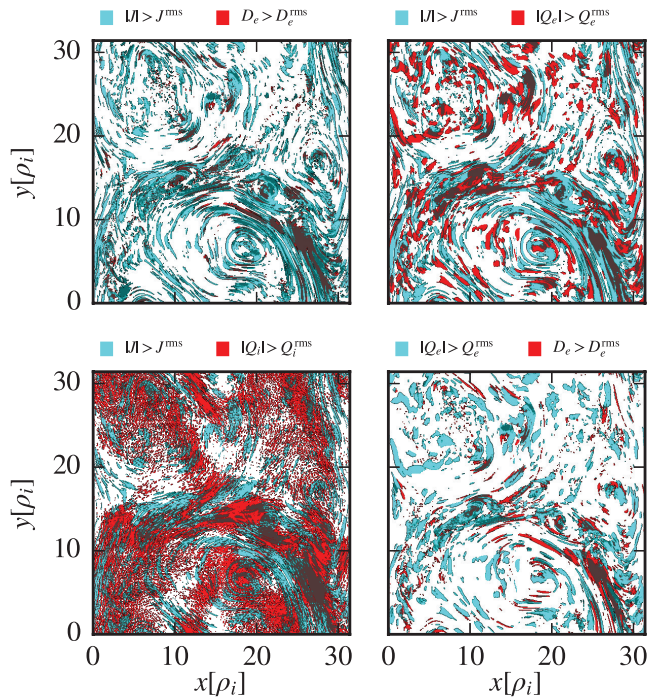

FIG. 3. (Color online) Superposition of two different fields for values larger than their RMS values. Matching values are shown with dark color (gray).

from Fig. 2. The amount of electron heating contained in current sheets is just 35% of the total space-integrated value. The same comparison for Q_i yields 30% and 65% for $D_e > 0$. Restricting the analysis to intense heating structures above the RMS value (Fig. 3), we find that only 45% of Q_e and 35% of Q_i peaks are in current sheets. Not only is the heating not dominated by intense value structures, but these structures fall mostly outside current sheets. The same analysis for D_e yields 90%. These results agree with previous findings, where it was shown that EFDM was predominantly concentrated in current sheets [10, 13]. Regarding the comparison of D_e and Q_e, only 25% of high Q_e values match the high values of D_e. We have also verified that the agreement between Q_e and D_e does not significantly improve by choosing a lower threshold to define intense peaks in D_e.

Finally, to better gauge how the EFDM and heating structures are distributed in space and in current sheets we employ a series of diagnostics, similar to the ones introduced in Ref. [10] and employed for the analysis of D_e. For a field F with a total volume V, we define the volume V_F as the volume occupied by values of $|F|$ larger than $\lambda F^{\max}$, where $F^{\max}$ is the maximal absolute value of F at any (x, y, z) point and $\lambda \in [0, 1]$. In Fig. 4(a) we plot the volume filling ratios V_F/V versus λ. We see that high intensity heating structures (with respect to their maximal value) occupy a much larger volume than D_e, the latter showing a very good agreement with

the filling ratio of J^2. Fig. 4(b) compares the PDFs of $|Q_e|$, $|Q_i|$, D_e, and J^2. D_e has the broadest distribution, which is again closer to the distribution of J^2, while Q_e and Q_i have a much narrower distribution. These results clearly show that the EFDM cannot be considered as representative for turbulent heating in weakly collisional plasmas. An explanation can be given in terms of the cascade through phase space. D_e represents only an injection of electromagnetic energy into the cascade and agrees very closely with the locations of current sheets. The injection of energy and (irreversible) dissipation generally form a causal relationship. Energy transfer from fields to particles is necessary for dissipation to occur, however, when collisions are rare, the conversion of free energy into heat need not happen at the same time as the actual transfer. In particular, the fluctuations are advected through phase space from the point where energy transfer occurs to the point where velocity gradients are sufficiently large for the collisional term to become significant. Once the free energy reaches the smallest scales at a later time, it is no longer confined to current sheets. For solar wind turbulence, our result could be modified when considering the role of inertial range dynamics. In a simulation with a better resolved inertial range, the increased level of intermittency may give rise to more pronounced non-Maxwellian features around the most intense current sheets. These features are beyond the scope of the present work, where fluctuations in the distribution function are assumed to be small and the simulation box covers only the tail of the inertial range.

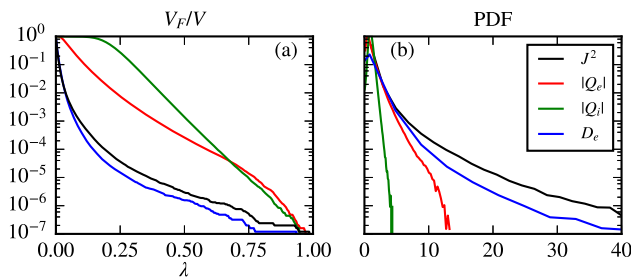*Plasma heating channels.*— As shown above, the real space

FIG. 4. (Color online) (a) Volume filling ratio (see text) and (b) PDFs comparing the behavior of $|Q_e|$, $|Q_i|$, and D_e. The J^2 curves are displayed for reference, showing a good agreement with D_e.

FIG. 5. (Color online) Normalized perpendicular wavenumber spectra for electron and ions heating rates. The parallel electron and perpendicular ion contributions to the heating rate are shown for comparison. Curves are multiplied by $k_\perp$ so the area under the curve (in log scale for $k_\perp$) is proportional to the collisional dissipation rate.

structure of ion and electron heating differs. To gain insight into the heating route preferred for each species, we split the collisional dissipation into the following contributions:

$$Q_\sigma = Q_\sigma^\parallel + Q_\sigma^\perp + Q_\sigma^{\text{coupling}}, \qquad (3)$$

where $Q_\sigma^\parallel$ involves only the parallel velocity derivatives of $C[f_\sigma]$, $Q_\sigma^\perp$ involves only the magnetic moment μ derivatives and contains a $[k_\perp \rho_\sigma]^2$ spatial term due to the GK transformation of the particle perpendicular velocity, and $Q_\sigma^{\text{coupling}}$ is a coupling term which involves the product of both parallel and perpendicular velocity derivatives (see Supplemental Material [33]). As the collisional term $C[f_\sigma]$ has the same form for both ions and electrons, observing a dominance of $Q_\sigma^\parallel$ or $Q_\sigma^\perp$ implies that smaller parallel or perpendicular velocity structures are preferentially developed. The development of parallel velocity structures is due to linear phase mixing and indicates a predilection for Landau damping. The results are shown in Fig. 5. The electron collisional dissipation (Q_e) spectrum peaks at low $k_\perp$. This hints that Landau damping is the preferred route for electron heating [8], for which linear phase mixing is crucial, as discussed in Refs. [37, 38] for weakly collisional reconnection in two dimensions. For Alfvénic turbulence addressed in the present Letter, the importance of electron Landau resonance and linear phase mixing is clearly shown by the fact that Q_e is dominated by the $Q_e^\parallel$ contribution (approximately 96% of the total electron heating), a result possible only due to the presence of strong parallel velocity gradients. By comparison, the ion free energy is cascaded to small perpendicular scales and dissipated around $k_\perp \rho_i \sim 25$. Approximately 80% of the total ion free energy is dissipated solely due to the $Q_i^\perp$ contribution. The main ion heating channel is therefore nonlinear phase mixing, the latter being characterized by the simultaneous generation of small perpendicular velocity and spatial structures [39], in contrast to linear Landau damping which effects the parallel velocity structure.

Discussion and conclusions— In this Letter, we analyzed the relation between turbulent heating rates and current sheets in a weakly collisional plasma by comparing directly both quantities in real space. Using gyrokinetic simulations of KAW turbulence, we obtaine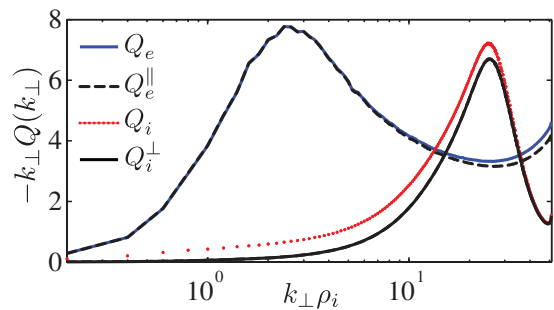d evidence that the locations of current sheets (defined as regions of high current) do not generally correspond to peaks in the electron and ion heating rates. Several authors have previously argued that heating in the solar wind occurs mainly in current sheets. However, one needs to take into account that these analyses were performed either by using various dissipation proxies instead of the actual local heating rates [7–10, 13] or without measuring directly the heating rate in real space [8]. Indeed, when comparing D_e with the electric current, we find a good agreement between these quantities, but not between J (or D_e) and the electron and ion heating rates. Furthermore, using gyrokinetic simulations of KAW turbulence, we showed that plasma heating is highly anisotropic in velocity space, providing first time direct measurements that identify the dominant collisional direction for each species. We identified Landau damping as the preferred route for the electron heating, while nonlinear (perpendicular) phase mixing is the channel responsible for ion heating. These results demonstrate the importance of kinetic dynamics and the use of well-defined collisional dissipation measures for studying plasma heating, further stressing the need for in-situ spacecraft measurements that would allow precise estimates of collisional heating from particle distribution functions.

* banon@physics.ucla.edu

† bogdan.teaca@coventry.ac.uk

[1] J. D. Richardson and C. W. Smith, Geophys. Res. Lett. **30**, 1206 (2003).

[2] R. Bruno and V. Carbone, Living Rev. Solar Phys. **10**, 2 (2013).

[3] D. Verscharen, E. Marsch, U. Motschmann, and J. Müller, Phys. Plasmas **19**, 022305 (2012).

[4] O. Chang, S. P. Gary, and J. Wang, Phys. Plasmas **21**, 052305 (2014).

[5] S. Servidio, F. Valentini, D. Perrone, A. Greco, F. Califano, W. H. Matthaeus, and P. Veltri, J. Plasma Phys. **81**, 325810107 (2015).

[6] D. Told, F. Jenko, J. M. TenBarge, G. G. Howes, and G. W. Hammett, Phys. Rev. Lett. **115**, 025003 (2015).

[7] T. N. Parashar, S. Servidio, M. A. Shay, B. Breech, and W. H. Matthaeus, Phys. Plasmas **18**, 092302 (2011).

[8] J. M. TenBarge and G. G. Howes, Astrophys. J. Lett. **771**, L27 (2013).

[9] H. Karimabadi, V. Roytershteyn, M. Wan, W. H. Matthaeus, W. Daughton, P. Wu, M. Shay, B. Loring, J. Borovsky, E. Leonardis, S. C. Chapman, and T. K. M. Nakamura, Phys. Plasmas **20**, 012303 (2013).

[10] M. Wan, W. H. Matthaeus, H. Karimabadi, V. Roytershteyn, M. Shay, P. Wu, W. Daughton, B. Loring, and S. C. Chapman, Phys. Rev. Lett. **109**, 195001 (2012).

[11] B. J. Vasquez, S. A. Markovskii, and B. D. G. Chandran, Astrophys. J. **788**, 178 (2014).

[12] R. S. Hughes, S. P. Gary, and J. Wang, Geophys. Res. Lett. **41**, 8681 (2014).

[13] M. Wan, W. H. Matthaeus, V. Roytershteyn, H. Karimabadi, T. Parashar, P. Wu, and M. Shay, Phys. Rev. Lett. **114**, 175002 (2015).

[14] E. Leonardis, L. Sorriso-Valvo, F. Valentini, S. Servidio, V. Carbone, and P. Veltri, Phys. Plasmas **23**, 022307 (2016).

[15] S. P. Gary, R. S. Hughes, and J. Wang, Astrophys. J. **816**, 102 (2016).

[16] A. Retino, D. Sundkvist, A. Vaivads, F. Mozer, M. Andre, and C. J. Owen, Nat. Phys. **3**, 236 (2007).

[17] D. Sundkvist, A. Retinò, A. Vaivads, and S. D. Bale, Phys. Rev. Lett. **99**, 025004 (2007).

[18] K. T. Osman, W. H. Matthaeus, A. Greco, and S. Servidio, Astrophys. J. Lett. **727**, L11 (2011).

[19] K. T. Osman, W. H. Matthaeus, B. Hnat, and S. C. Chapman, Phys. Rev. Lett. **108**, 261103 (2012).

[20] S. Perri, M. L. Goldstein, J. C. Dorelli, and F. Sahraoui, Phys. Rev. Lett. **109**, 191101 (2012).

[21] D. Perrone, O. Alexandrova, A. Mangeney, M. Maksimovic, C. Lacombe, V. Rakoto, J. C. Kasper, and D. Jovanovic, Astrophys. J. **826**, 196 (2016).

[22] J. J. Podesta, Solar Phys. **286**, 529 (2013).

[23] S. Boldyrev, C. H. K. Chen, Q. Xia, and V. Zhdankin, Astrophys. J. **806**, 238 (2015).

[24] C. L. Vásconez, F. Pucci, F. Valentini, S. Servidio, W. H. Matthaeus, and F. Malara, Astrophys. J. **815**, 7 (2015).

[25] G. G. Howes, Phil. Trans. R. Soc. A **373** (2015).

[26] A. J. Brizard and T. S. Hahm, Rev. Mod. Phys. **79**, 421 (2007).

[27] D. Told, J. Cookmeyer, F. Muller, P. Astfalk, and F. Jenko, New J. Phys. **18**, 065011 (2016).

[28] F. Jenko, W. Dorland, M. Kotschenreuther, and B. N. Rogers, Phys. Plasmas **7**, 1904 (2000).

[29] J. TenBarge, G. Howes, W. Dorland, and G. Hammett, Comput. Phys. Commun. **185**, 578 (2014).

[30] U. Frisch, *Turbulence. The legacy of A. N. Kolmogorov* (Cambridge University Press, Cambridge, UK, 1995).

[31] G. G. Howes, S. C. Cowley, W. Dorland, G. W. Hammett, E. Quataert, and A. A. Schekochihin, Astrophys. J. **651**, 590 (2006).

[32] L. D. Landau, Phys. Z. Sowjet. **10**, 154 (1936), translated in The transport equation in the case of Coulomb interactions, *Collected Papers of L. D. Landau* (Pergamon Press, Oxford, 1965).

[33] See Supplemental Material at [URL will be inserted by publisher] for an explicit form of the collision operator implemented in GENE.

[34] O. Pezzi, F. Valentini, and P. Veltri, J. Plasma Phys. **81** (2015).

[35] O. Pezzi, F. Valentini, and P. Veltri, Phys. Rev. Lett. **116**, 145001 (2016).

[36] S. Zenitani, M. Hesse, A. Klimas, and M. Kuznetsova, Phys. Rev. Lett. **106**, 195003 (2011).

[37] N. F. Loureiro, A. A. Schekochihin, and A. Zocco, Phys. Rev. Lett. **111**, 025002 (2013).

[38] R. Numata and N. F. Loureiro, J. Plasma Phys. **81**, 305810201 (2015).

[39] A. A. Schekochihin, S. C. Cowley, W. Dorland, G. W. Hammett, G. G. Howes, E. Quataert, and T. Tatsuno, Astrophys. J. Suppl. Ser. **182**, 310 (2009).